Effects of nanoscale embedded Schottky barriers on carrier dynamics in ErAs:GaAs composite systems

S. N. Gilbert Corder, J. K. Kawasaki, C. J. Palmstrøm, H. T. Krzyżanowska, and N. H. Tolk

Phys. Rev. B **92**, 134303 — Published 5 October 2015

DOI: 10.1103/PhysRevB.92.134303

Effects of Nanoscale Embedded Schottky Barriers on Carrier Dynamics in ErAs:GaAs Composite Systems

S. N. Gilbert Corder,[1,2,*] J. K. Kawasaki,[3,4] C. J. Palmstrøm,[3,5] H. T. Krzyżanowska,[6] and N. H. Tolk[6]

[1] *Interdisciplinary Materials Science Program, Vanderbilt University, Nashville, TN, USA*
[2] *Current address: Department of Physics and Astronomy, Stony Brook University, Stony Brook, NY*
[3] *Materials Department, University of California Santa Barbara, Santa Barbara, CA, USA*
[4] *Current address: Kavli Institute at Cornell for Nanoscale Science and Laboratory for Atomic and Solid State Physics, Cornell University, Ithaca, NY*
[5] *Department of Electrical Engineering, University of California Santa Barbara, Santa Barbara, CA, USA*
[6] *Department of Physics and Astronomy, Vanderbilt University, Nashville, TN, USA*

(Dated: September 18, 2015)

Semiconducting GaAs is widely used in microwave and millimeter integrated circuits, infrared LEDs, lasers, and solar cells. Introducing semi-metallic ErAs nanoparticles provides a way to controllably tune the optical and electronic properties of GaAs. We show for high volume fractions (0.5-10%) of ErAs nanoparticles embedded in GaAs, the relaxation dynamics indicate ErAs forms discrete states in the GaAs bandgap. For specific carrier momentum conditions, the localized Schottky states may be occupied, exhibit carrier trapping, or inject carriers into the GaAs conduction band. Carrier occupation and scattering from the Schottky states has not previously been reported in optical studies of this system. The scattering mechanism is observed to be active above an occupation threshold where the excited carrier density exceeds the trap density. The array of nanoparticle densities and the characterization of the relaxation pathways at multiple carrier excitation energies represents the most complete fundamental investigation of these systems to date.

GaAs is the material of choice for high speed photoconductive devices such as p-n junctions, solar cells, ultrafast optical switches, photomixers, and thermoelectric structures[1]. Hybridized metal nanostructure/GaAs systems controlled by ultrafast optical pulses can achieve much faster switching than is attainable by phase change, voltage-driven carrier injection, liquid crystals or the modulation of superconductivity[2]. Interest in the embedded nanoparticle ErAs:GaAs composite system stems from the ability to control the optical and electronic properties of GaAs by incorporating semimetallic ErAs nanoparticles without altering the position of the GaAs bandgap[3] and retaining high quality, atomically sharp ErAs/GaAs interfaces[4,5]. The composite systems display tunable photo-carrier relaxation with ultrashort relaxation times spanning two orders of magnitude[3,6], while achieving greater film quality[1,7–9] and transport characteristics than low temperature grown GaAs[1,10–16]. These features have made the ErAs:GaAs system highly promising for integration into GaAs-based opto-electronic devices[6,14,17–21]. However, the fundamental relaxation phenomena of these systems must be fully characterized before such applications can be realized.

To date, characterization of the relaxation dynamics in ErAs:GaAs composites has focused on optimizing ultrashort relaxation times in superlattice structures with low ErAs volume fractions as such systems show promise for THz device applications. These studies utilize the bonding differences between the ErAs rocksalt and GaAs zinc blende crystal structures, which introduce localized trap states into the bandgap of GaAs[13,22]. The trap states act as non-radiative recombination sites for photo-excited GaAs carriers[3,6,23,24], and carrier trapping times are altered by varying superlattice spacing[3,23].

The following work presents the observation of carrier absorption, occupation and scattering from embedded Schottky barriers in the ultrafast response of single $ErAs_x$:$GaAs_{1-x}$ layers where the ErAs is randomly distributed in the GaAs matrix, and the volume fraction of ErAs is large-ranging from $x = 0.5 - 10\%$. These dynamical processes have not previously been reported in other studies of the composite ErAs:GaAs systems. The carrier dynamics are characterized for three photon energies and indicate that the ultrafast response is highly sensitive to carrier occupation of the Schottky interface states, carrier momentum, carrier density, and availability of the trap states.

In this paper, six composite samples with different volume fractions of ErAs nanoparticles embedded in a GaAs matrix are studied, along with a commercially available undoped semi-insulating GaAs reference sample. Each composite sample consists of a semi-insulating GaAs $\langle 001 \rangle$ substrate; 250 nm GaAs buffer; 300 nm of randomly distributed $ErAs_x$:$GaAs_{1-x}$ embedded nanoparticle layer grown by simultaneous co-deposition of Er, Ga and As; followed by a 10 nm GaAs capping layer to prevent oxidation (see the inset of Figure 1a). The composite layers have ErAs volume fractions of x = 0 to 10%. For more information on the growth process, please see the Supplemental Material at [URL will be inserted by publisher].

The relative static absorption of the samples is shown in Figure 1a for the GaAs fundamental absorption edge and band tails at 300 K. The GaAs bandgap at room-temperature is indicated by the dashed vertical line at 1.42 eV. The x = 0% $ErAs_x$:$GaAs_{1-x}$ sample displays a softening of the band edge with respect to the commercial GaAs reference, but otherwise shows no distinct

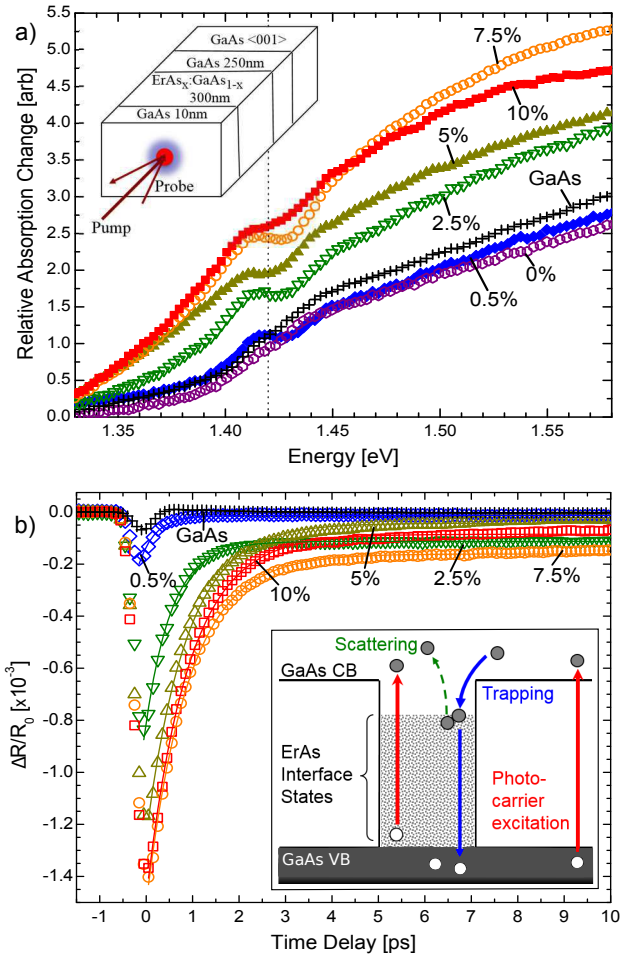

FIG. 1. Static absorption, schematic of system dynamics, sample configuration and trapping time characterization of the $ErAs_x$:$GaAs_{1-x}$ composite system. a) Relative static absorption obtained by ellipsometry for $ErAs_x$:$GaAs_{1-x}$ with x = 0-10% and intrinsic GaAs, vertically offset for clarity. The dashed vertical line indicates the location of the room temperature conduction band edge of GaAs at 1.42 eV. Significant absorption is observed in the ErAs-containing samples below the bandgap. Inset: Schematic of the sample structure and time-resolved experimental geometry. b) Differential reflectivity response at 1.38 eV for x = 0.5-10% volume fractions of $ErAs_x$:$GaAs_{1-x}$ and the GaAs reference for a pump fluence of approximately 13 μJ/cm^2 at 1.38 eV. The solid lines are exponential fits used to extract the time constants. Inset: 1D cut through the ErAs nanoparticle and GaAs matrix illustrating proposed dynamics in the composite system where the conduction band (CB) and valence band (VB) of GaAs are shown and the ErAs/GaAs interface gives rise to a localized trap states within the bandgap. The shaded areas indicate electron occupation and the arrows illustrate the dynamic carrier processes. The red arrows indicate photo-excitation, while the blue arrows (trapping) and green arrow (scattering) indicate pathways introduced by the interface states.

difference in absorption properties. An absorption peak within the band tails is observed in the ErAs-containing samples in Figure 1a. These absorption features, noticeably absent in either the 0% or GaAs reference spectra, arise from the incorporation of the ErAs nanoparticles. The slope of the band tails is also observed to increase with ErAs volume fraction (a figure of the band tail slopes can be found in the Supplemental Material), indicating an increase in the density of interface states with ErAs incorporation. The interface between metallic ErAs and semiconducting systems are known to create localized traps, or Schottky barriers[14,21,25,26], with different barrier heights depending on the crystallographic directions of the interface[27]. The interface states are partiality occupied and extend into the GaAs matrix[13,22], providing a route for the carriers to move from the interface into the GaAs host. The absorption data suggest the Schottky states formed at the interface can be photo-excited at sub-bandgap energies, contributing carriers to the conduction band. The presence of these interface states and their effects on the dynamics of the system are presented and discussed below.

A diagram of the proposed system dynamics in the vicinity of an ErAs nanoparticle based on the experimental results can be seen in the inset of Figure 1b. Carriers excited into the conduction band either relax through typical GaAs photo-carrier decay channels[28], or can be captured by the trap state and non-radiatively recombine. Carriers populating the interface state may be photo-excited into the GaAs conduction band, non-radiatively recombine, or scatter into the GaAs conduction band from occupied interface states. As the volume fraction of ErAs increases, the density of interface states likewise increases.

The relaxation dynamics are studied via degenerate time resolved pump-probe reflectivity (PPR) measurements at room temperature for three photon energies: 1.38, 1.46, and 1.55 eV to characterize the behavior of the composite systems below, near and above the GaAs bandgap (E_g =1.42 eV). The intrinsic GaAs response at each photon energy is shown as a reference. The probe fluence is held constant at 0.5 μJ/cm^2 throughout all measurements. The PPR signal is given as the relative change in reflectivity induced by the pump pulse with respect to the background reflectivity measured by the probe ($\frac{\Delta R}{R_0}$) with a signal strength on the order of 10^{-3}. Data are fit using multiple exponential functions to extract time constants, with the error bars as indicators of fit uncertainty.

Figure 1b shows the experimental PPR of the GaAs reference and $ErAs_x$:$GaAs_{1-x}$ systems photo-excited at 1.38 eV, below the GaAs bandgap. Excitation below the bandgap produces a negative PPR response[28,29], and the small GaAs transient is the result of excited defects or surface states which decay nearly instantaneously within the measurement resolution. The ErAs-containing sample responses are characterized as a single sharp negative peak followed by an exponential decay. The ErAs responses are significantly longer lived than the GaAs reference, and increasingly negative with ErAs incorporation. Time-resolved conductivity measurements of

ErAs:GaAs superlattice composites have indicated GaAs photo-carriers are captured by the interface states within a few ps of excitation[23]. Further, the trapping times vary with ErAs-incorporated layer spacing, suggesting that decreasing the distance between ErAs nanoparticles decreases the amount of time excited carriers travel before being captured by the interface states[3,6,23,24]. As the excitation energy is not sufficient to excite carriers across the GaAs bandgap, the initial response at zero time delay is the result of carriers excited from the interface states into the GaAs conduction band being captured by the traps. The magnitude of the PPR response at 1.38 eV further reinforces the correlation between the density of interface trap states and the ErAs volume fractions observed in the absorption data: the higher volume fractions have more partially occupied interface states capable of being photoexcited.

Figure 2 shows the response of each sample excited above the GaAs conduction band edge at 1.46 and 1.55 eV. The response of the ErAs:GaAs composites changes significantly with photo-excitation energy. At both excitation energies, the ErAs-containing samples show evidence of the negative carrier trapping signatures[3], followed by a positive rise. At 1.46 eV the positive rise appears to be recovery of the system to pre-pump conditions; while at 1.55 eV the positive rise is more pronounced and no longer appears to be a simple recovery.

The PPR response of the GaAs reference at 1.46 eV is characterized by the slow exponential decay of excited carrier populations, indicative of carrier and lattice thermalization processes in the conduction band[28,29]. The $ErAs_x$:$GaAs_{1-x}$ responses show markedly different behavior from the GaAs reference within the first few ps of photo-excitation. Except for the 0.5%, the ErAs containing systems all display a negative trapping signature following photo-excitation, indicating GaAs carriers are excited directly into the interface trap states. The 0.5% system exhibits GaAs-like excitation, followed by a slow negative transient at longer time delays. The positive peak at short time delays suggests the traps states may be initially saturated during photo-excitation, requiring several ps for the traps to empty and the excited carrier population to be reduced. The negative maxima of the 7.5 and 10% volume fractions slowly evolve with an exponential behavior toward the pre-excitation reflectivity values, indicating the trap density is sufficient to capture the excited photo-carriers. Following the trapping signature for the 2.5 and 5% systems, the systems recover slowly to pre-excitation values. The PPR response of the 5% volume fraction is smaller than the other samples at this excitation energy and is likely a result of the lower index of refraction of this sample at 1.46 eV; see the Supplemental Material for more information.

Photo-excitation at 1.55 eV is shown in Figure 2b. The fast bi-exponential decay of the GaAs reference is a result of carrier-carrier scattering and optical phonon emission, followed by thermalization[28,29]. All of the composite samples studied initially display carrier excitation into the GaAs conduction band followed by a negative signature and a slower positive contribution at longer delay times. The negative transient at 1.55 eV is attributed to a rapid decrease in the excited carrier population as a result of trapping, consistent with previous studies at this excitation energy[3,23]. The 0.5% sample has a weak trapping signature that gives way to a positive rise after 5 ps. The 2.5% response shows a sharp trapping signature followed by a strong positive rise which peaks in the middle of the time window before decaying. The 5-10%

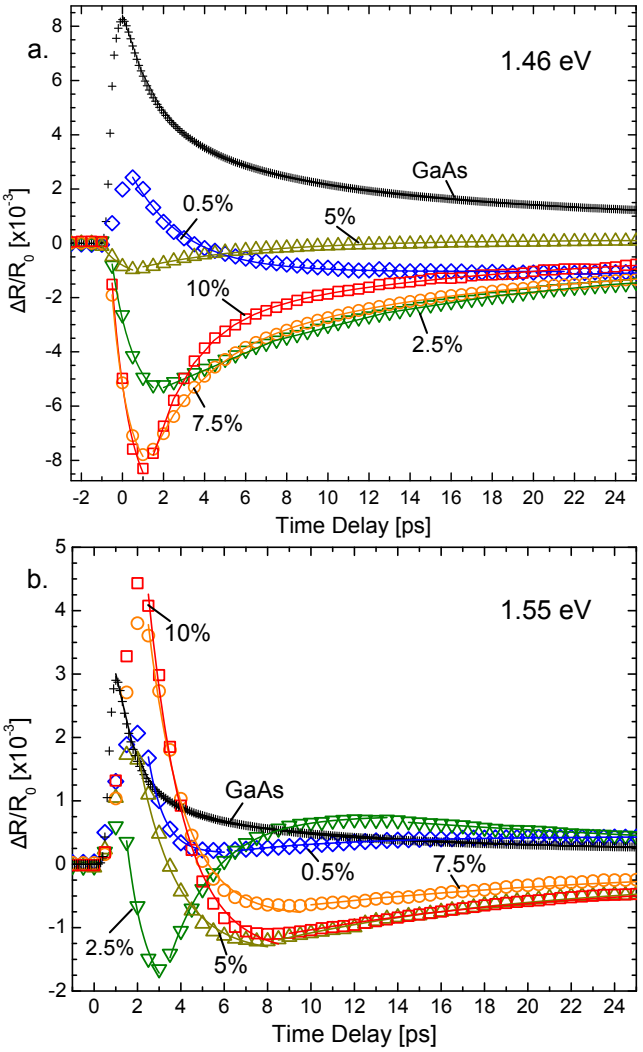

FIG. 2. Differential reflectivity response for x = 0.5-10% volume fractions of $ErAs_x$:$GaAs_{1-x}$ and the GaAs reference for a pump fluence of approximately 15 $\mu J/cm^2$ at a) 1.46 and b) 1.55 eV. The solid lines are exponential fits used to extract the time constants. The carrier dynamics in the GaAs reference response are faster at 1.55 eV compared to 1.46 eV as a result of carrier-carrier scattering and optical phonon emission redistributing energy more effectively than acoustic phonon emission. The ErAs-containing samples display faster carrier trapping times and the higher volume fractions also recover faster at 1.55 eV. For the 0.5 and 2.5%, the extra carrier momentum and density slow the recovery process.

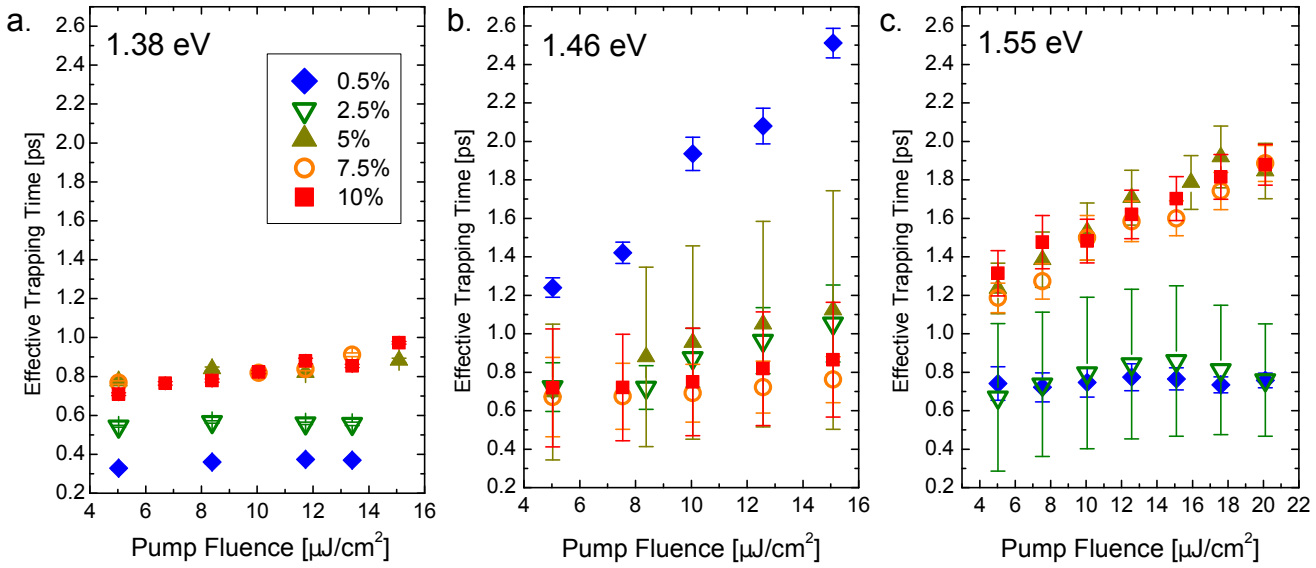

FIG. 3. The effective carrier trapping times for the ErAs samples as a function of pump fluence for the $ErAs_x$:$GaAs_{1-x}$ composite system at a) 1.38 eV, b) 1.46 eV and c) 1.55 eV. a) The trapping times of the 0.5 and 2.5% volume fractions display no carrier density (fluence) dependence, indicating the trap density is larger than the interface state carrier density. In contrast, the 5-10% volume fractions show an increase in trapping time with fluence, suggesting the excited interface state carrier density is greater than the trap density. b) For excitation at 1.46 eV, the 0.5-5% samples exhibit trap saturation. For the 0.5% sample, excess carriers occupy the GaAs conduction band resulting in marked increases in carrier capture time as the carrier density increases. The 7.5 and 10% volume fractions show no significant change with respect to the effective trapping times observed at 1.38 eV. c) Excitation at 1.55 eV results in carrier relaxation through the GaAs conduction band, producing effective trapping times which are significantly longer for the 5-10% volume fractions and show a strong carrier density dependence. The effective trapping times of the 0.5 and 2.5% volume fractions display little variation and are shorter than those observed at 1.46 eV: the traps are no longer saturated.

volume fractions show similar responses where the trapping signature gives way to a positive rise at longer time delays. The positive reflectivity contributions at longer time delays could be the result of electron injection from the embedded metallic structures to the semiconducting host conduction band[1,30], resulting in carrier movement to higher energy levels in an Auger-like scattering process. The influence of trap density versus carrier density on the observed dynamics will be further explored below.

The effective trapping times at the three photon energies studied are shown in Figure 3, and are consistent with the reported trapping times similar systems[3,6,23,24]. Intrinsic trapping times below 190 fs have been reported for ErAs:GaAs[6]; therefore, the observed effective trapping times are the convolution of excited carrier capture and trap emptying through non-radiative recombination. Increases in trapping times with pump fluence are attributed to trap saturation when carrier density exceeds trap density[24].

At 1.38 eV, the effective trapping times of the 5-10% volume fractions show a clear increase in trapping time with pump fluence, while the effective trapping times of the 0.5 and 2.5% volume fractions are relatively unchanged. Since the excitation energy is below the GaAs bandgap, these measurements suggest that the carriers present in the interface states of the 0.5 and 2.5% samples are being fully excited at these fluences and the trap density is larger than the interface state carrier density. In contrast, the 5-10% trapping times increase with fluence, suggesting the trap states are saturating as more carriers are available for photo-excitation in the interface states at higher volume fractions. For the high volume fractions, the excited interface state carrier density exceeds the trap density. This is consistent with Figure 1a, in which increased absorption is observed for the 5-10% volume fractions compared to the low volume fractions.

As the excitation energy increases from 1.38 to 1.46 eV, GaAs carriers are excited in addition to interface state carriers. The effective carrier trapping times of the 0.5-2.5% volume fractions significantly increase and exhibit pump fluence dependence. This behavior has previously been attributed to trap saturation, where excited carriers remain in the GaAs until the trap state is available[23]. For the 0.5% sample, the carriers waiting to be captured by the trap states give rise to the positive PPR response observed in Figure 2a, suggesting the interface states are fully occupied. The 2.5 and 5% samples show slight increases in trapping time at higher pump fluences with respect to 1.38 eV, but still maintain the trapping signature in the PPR response, indicating the excited carriers occupy the interface states while waiting to recombine. The 7.5 and 10% show no significant change in trapping

time within the error of the measurements and the PPR response at 1.46 eV deviates little from that observed at 1.38 eV: the density of the interface states is sufficient to accommodate the GaAs photo-carriers.

The effective carrier trapping times at 1.55 eV show the same general trends as those observed at 1.38 eV, but are significantly longer as a result of carrier relaxation through the GaAs conduction band states before trapping. For the high volume fractions (5-10%), the excited carriers remain in the GaAs conduction band while waiting to be trapped; increasing the effective trapping time with higher carrier densities. For the 0.5 and 2.5% systems, the effective trapping times show no clear fluence dependence and are shorter than those observed at 1.46 eV, implying the excess carriers are not simply waiting to be trapped but are involved in another dynamical process. It is clear from looking at the PPR spectra of the 0.5 and 2.5% at 1.55 eV that carriers appear to be repopulating the GaAs conduction band rather than waiting in low energy states to be trapped.

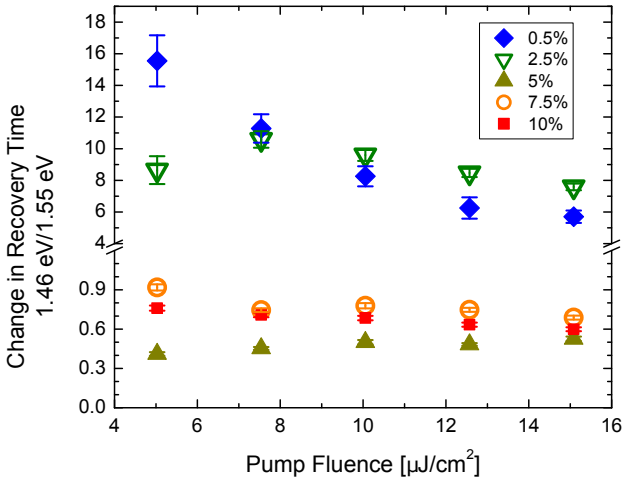

FIG. 4. The change in recovery time (1.45 eV/1.55 eV) as a function of pump fluence for the $ErAs_x$:$GaAs_{1-x}$ composite systems. The 5-10% volume fractions display longer recovery times at higher excitation energies and little fluence dependence: the recovery process is slower for higher carrier momentum. The recovery times for the 0.5 and 2.5% volume fractions are significantly shorter at the higher excitation energy and the recovery times are the shortest for the highest photo-carrier densities (fluences). The decrease in recovery time with increased carrier momentum and density suggest the carriers are utilizing another relaxation pathway.

The PPR spectra for excitations above the bandgap are characterized by a negative trapping transient and a subsequent positive rise. These positive contributions are compared in Figure 4 as ratios of the extracted recovery time constants at 1.46 eV to those at 1.55 eV for the ErAs-containing samples. The recovery time of the 5-10% volume fractions is observed to increase at the higher excitation energy with little influence from photo-carrier density (fluence). Carrier trapping is the major dynamic process observed in the PPR response of the high volume fraction samples and the increase in carrier momentum slows the recovery process, increasing the time for carriers at the interface to relax through the trap states. A different trend is observed for the recovery time of 0.5 and 2.5% volume fractions. The PPR spectra of the 0.5 and 2.5% volume fractions at 1.55 eV display a positive rise beyond the recovery signal of the other samples: the reflectivity values exceed the pre-excitation values at long time delays. The recovery times for these two systems at 1.55 eV are significantly shorter than what is observed at 1.46 eV and recovery happens most quickly at the highest photo-carrier densities (fluences). The trapping time constants in Figure 3 for these two samples indicate the trap states are saturated at 1.46 eV but not at 1.55 eV. The decrease in recovery time with increased carrier momentum and density, combined with the positive PPR response at long time delays suggests the carriers are utilizing another energetic pathway: given sufficient momentum and density, the excited carriers scatter back into the GaAs conduction band.

Considering the static absorption, PPR, fluence and energy dependent characteristic times, the following picture of the ErAs:GaAs system emerges. Below the bandgap, photo-carrier excitation of the interface states results in a population of carriers in the GaAs conduction band which are rapidly trapped. For low volume fractions, the trap density exceeds the interface state carrier density, producing nearly constant trapping times as pump fluence is changed. In contrast, higher volume fractions exhibit increased trapping times as carrier density increases, indicating the excited interface state carrier density is larger than the trap density. At 1.46 eV, carriers are excited primarily from the GaAs host into the available interface states, populating the conduction band edge if the traps states are occupied. The recovery of the composite systems depends on the availability of the trap states, with higher volume fractions recovering more rapidly. Carriers are excited high into the GaAs conduction band at 1.55 eV and are rapidly captured by the interface traps. The high carrier momentum and occupation of the interface traps induces carrier scattering from the trap states to the GaAs conduction band when the carrier density exceeds the trap density.

In summary, the incorporation of semi-metallic ErAs during the growth of GaAs produces nanoparticles with partially occupied interface states that extend into the GaAs bandgap. These states are capable of being occupied and excited, in addition to providing traps for rapid carrier relaxation. The dynamics associated with the presence of these states depend highly on the excitation energy and density of the carriers as well as the density of interface states. This work represents the most comprehensive study of the relaxation dynamics of single-layer ErAs:GaAs composites to date.

The unique optical properties of ErAs:GaAs composites suggest such systems can be used for adaptive, highly tailored structures where the injection and depletion of

carriers is optically controlled[2] and unwanted carrier dynamics can be swept out through biasing. Flexibility in the growth process could prevent stark interfaces and thereby improve charge transfer, lower resistivity, and tune barrier heights. Specific volume fraction devices could be used for photon detection at discrete energies or for carrier density detection. However, detailed knowledge of carrier dynamics is a critical preliminary step in order for ErAs:GaAs composite applications to be realized.

ACKNOWLEDGMENTS

The authors would like to acknowledge the following funding agencies for support: DoE contract number DE-FG02-99ER45781 and ARO contract number W911NF-14-1-0290. Portions of this work were completed using the shared resources of the Vanderbilt Institute of Nanoscale Science and Engineering (VINSE) core laboratories.

* Stephanie.GilbertCorder@StonyBrook.edu

[1] D. C. Driscoll, M. Hanson, C. Kadow, and A. C. Gossard, Appl. Phys. Lett. **78**, 1703 (2001).
[2] N. I. Zheludev and Y. S. Kivshar, Nat. Mater. **11**, 917 (2012).
[3] C. Kadow, S. B. Fleischer, J. P. Ibbetson, J. E. Bowers, A. C. Gossard, J. W. Dong, and C. J. Palmstrøm, Appl. Phys. Lett. **75**, 3548 (1999).
[4] D. O. Klenov, J. M. Zide, J. D. Zimmerman, A. C. Gossard, and S. Stemmer, Appl. Phys. Lett. **86**, 241901 (2005).
[5] N. Stoffel, C. Palmstrøm, and B. Wilkens, Nucl. Instrum. and Meth. B. **56-57, Part 2**, 792 (1991).
[6] M. Griebel, J. H. Smet, D. C. Driscoll, J. Kuhl, C. A. Diez, N. Freytag, C. Kadow, A. C. Gossard, and K. von Klitzing, Nat. Mater. **2**, 122 (2003).
[7] H.-K. Jeong, T. Komesu, C.-S. Yang, P. Dowben, B. Schultz, and C. Palmstrøm, Mater. Lett. **58**, 2993 (2004).
[8] T. E. Buehl, J. M. LeBeau, S. Stemmer, M. A. Scarpulla, C. J. Palmstrøm, and A. C. Gossard, J. Cryst. Growth **312**, 2089 (2010).
[9] J. K. Kawasaki, R. Timm, T. E. Buehl, E. Lundgren, A. Mikkelsen, A. C. Gossard, and C. J. Palmstrøm, J. Vac. Sci. Technol., B **29**, 03C104 (2011).
[10] E. R. Brown, A. Bacher, D. Driscoll, M. Hanson, C. Kadow, and A. C. Gossard, Phys. Rev. Lett. **90**, 077403 (2003).
[11] P. Pohl, F. H. Renner, M. Eckardt, A. Schwanhuer, A. Friedrich, A. Yksekdag, S. Malzer, G. H. Dhler, P. Kiesel, D. Driscoll, M. Hanson, and A. C. Gossard, Appl. Phys. Lett. **83**, 4035 (2003).
[12] S. Sethi and P. K. Bhattacharya, J. Electron. Mater. **25**, 467 (1996).
[13] K. T. Delaney, N. A. Spaldin, and C. G. Van de Walle, Phys. Rev. B **81**, 165312 (2010).
[14] J. M. O. Zide, A. Kleiman-Shwarsctein, N. C. Strandwitz, J. D. Zimmerman, T. Steenblock-Smith, A. C. Gossard, A. Forman, A. Ivanovskaya, and G. D. Stucky, Appl. Phys. Lett. **88**, 162103 (2006).
[15] R. Yano, Y. Hirayama, S. Miyashita, H. Sasabu, N. Uesugi, and S. Uehara, Phys. Lett. A **289**, 93 (2001).
[16] M. C. Beard, G. M. Turner, and C. A. Schmuttenmaer, J. Appl. Phys. **90**, 5915 (2001).
[17] K. W. Park, V. D. Dasika, H. P. Nair, A. M. Crook, S. R. Bank, and E. T. Yu, Appl. Phys. Lett. **100**, 233117 (2012).
[18] H. P. Nair, A. M. Crook, and S. R. Bank, Appl. Phys. Lett. **96**, 222104 (2010).
[19] M. A. Scarpulla, J. M. O. Zide, J. M. LeBeau, C. G. V. de Walle, A. C. Gossard, and K. T. Delaney, Appl. Phys. Lett. **92**, 173116 (2008).
[20] W. Kim, J. Zide, A. Gossard, D. Klenov, S. Stemmer, A. Shakouri, and A. Majumdar, Phys. Rev. Lett. **96**, 045901 (2006).
[21] K. J. Russell, I. Appelbaum, V. Narayanamurti, M. P. Hanson, and A. C. Gossard, Phys. Rev. B **71**, 121311 (2005).
[22] J. K. Kawasaki, R. Timm, K. T. Delaney, E. Lundgren, A. Mikkelsen, and C. J. Palmstrøm, Phys. Rev. Lett. **107**, 036806 (2011).
[23] R. P. Prasankumar, A. Scopatz, D. J. Hilton, A. J. Taylor, R. D. Averitt, J. M. Zide, and A. C. Gossard, Appl. Phys. Lett. **86**, 201107 (2005).
[24] A. K. Azad, R. P. Prasankumar, D. Talbayev, A. J. Taylor, R. D. Averitt, J. M. O. Zide, H. Lu, A. C. Gossard, and J. F. O'Hara, Appl. Phys. Lett. **93**, 121108 (2008).
[25] A. Dorn, M. Peter, S. Kicin, T. Ihn, K. Ensslin, D. Driscoll, and A. C. Gossard, Appl. Phys. Lett. **82**, 2631 (2003).
[26] J. D. Zimmerman, E. R. Brown, and A. C. Gossard, J. Vac. Sci. Technol. B **23**, 1929 (2005).
[27] C. J. Palmstrøm, T. L. Cheeks, H. L. Gilchrist, J. G. Zhu, C. B. Carter, B. J. Wilkens, and R. Martin, J.Vac. Sci. Technol. A **10**, 1946 (1992).
[28] J. Shah, *Ultrafast spectroscopy of semiconductors and semiconductor nanostructures*, Solid State Sciences (Springer-Verlag, Berlin, 1999).
[29] S. S. Prabhu and A. S. Vengurlekar, J. Appl. Phys. **95**, 7803 (2004).
[30] M. W. Knight, Y. Wang, A. S. Urban, A. Sobhani, B. Y. Zheng, P. Nordlander, and N. J. Halas, Nano Lett. **13**, 1687 (2013).